Proceedings of the ASME 2019
Dynamic Systems and Control Conference
DSCC2019
October 8-11, 2019, Park City, Utah, USA

DSCC2019-8996

A SERIES ELASTIC ACTUATOR DESIGN AND CONTROL IN A LINKAGE BASED HAND EXOSKELETON

Raghuraj J. Chauhan
Robotics and Mechatronics Lab
Department of Mechanical Engineering
Virginia Tech
Blacksburg, VA 24060
Email: raghur1@vt.edu

Pinhas Ben-Tzvi*
Robotics and Mechatronics Lab
Department of Mechanical Engineering
Virginia Tech
Blacksburg, VA 24060
Email: bentzvi@vt.edu

ABSTRACT

This paper presents the design of a series elastic actuator and a higher level controller for said actuator to assist the motion of a user's hand in a linkage based hand exoskeleton. While recent trends in the development of exoskeleton gloves has been to exploit the advantages of soft actuators, their size and power requirements limit their adoption. On the other hand, a series elastic actuator can provide compliant assistance to the wearer while remaining compact and lightweight. Furthermore, the linkage based mechanism integrated with the SEA offers repeatability and accuracy to the hand exoskeleton. By measuring the user's motion intention through compression of the elastic elements in the actuator, a virtual dynamic system can be utilized that assists the users in performing the desired motion while ensuring the motion stability of the overall system. This work describes the detailed design of the actuator followed by performance tests using a simple PD controller on the integrated robotic exoskeleton prototype. The performance of the proposed high level controller is tested using the integrated exoskeleton glove mechanism for a single finger, using two types of input motion. Preliminary results are discussed as well as plans for integrating the proposed actuator and high level controller into a complete hand exoskeleton prototype to perform intelligent grasping.

Keywords: Mechanism design, series elastic actuator, exoskeletons, human-machine interaction, motion planning

*Corresponding author

1 INTRODUCTION

A major source of disability is the lack of full functionality in ones hands. An estimated 4.19 million American adults reported difficulty grasping or handling small objects and 10.20 million reported difficulty lifting or carrying more than ten pounds as per the recent national survey in [1]. A frequent source of disability that could lead to this type of difficulty is stroke [2], with approximately five hundred thousand new stroke victims each year [3]. Much of the loss of grasping functionality comes from the improper muscle activation during individual finger motions leading to the inability to extend the fingers [4], potentially remedied by intensive rehabilitation.

Passive devices such as SaeboFlex [5] have been designed to assist the wearer in extending their digits after voluntary flexion. More intelligent, robotic approaches are being pursued and are of continued interest to the research community. This has lead to the almost ubiquitous development and integration of soft actuators for hand exoskeletons. Examples commonly fall into two categories based on pneumatic actuation of flexible membranes [6–10] and cable based transmission [11–14]. In pneumatic systems, the controllability can suffer from the lack of accurate measurements in the task space while requiring compressed air stored in tanks for operation. With regards to the cable driven approach, the wearer can experience discomfort from the tendon pre-loading and decreased efficiency due to frictional losses from contact along the cable routing [15]. Furthermore, both of these categories of system are large and sometimes heavy, which limits their usability.

With regards to the control of exoskeleton gloves, and

robotic exoskeletons in general, electromyography (EMG) sensors are often used to determine user intent [16]. However, the signal noise from EMG sensors is too large for direct determination of the desired operation and prolonged placement of these sensors becomes uncomfortable. Alternatively, EMG sensors can be placed at other locations on the body and those muscles can be used to control the exoskeleton at the cost of highly unintuitive operation. EMG based approaches can be coupled with vision based sensing to better estimate user intent [17, 18] with the drawback of requiring additional hardware and therefore an even larger operational setup.

In observation of both the unaddressed design and control challenges, this work presents a step towards intelligent control of a linkage based exoskeleton for those with partial hand mobility using series elastic actuators (SEAs). A compact SEA design is presented and integrated with a linkage based finger mechanism that is an evolution of the mechanism first presented in [19] with optimized kinematics from [20]. The compliant elements in the SEA allow the user to be comfortably assisted by the device and express their intent. The linkage system couples the motion of the metacarpophalangeal (MCP), proximal interphalangeal (PIP), and distal interphalangeal (DIP) joints in a highly compact form factor that sits entirely alongside the finger. While this work does not challenge the positive aspects of soft actuation, it aims to explore a novel hard linkage based approach, taking into account the distinct advantages in terms of force transmission and repeatability.

Numerous force control methods have been presented for robotic, lower extremity exoskeletons. While many of these methods seek to match the force of the actuator to its corresponding joint on the human body, a recent approach to amplify the force of the user is shown in [21] where positive feedback, coupled with a low pass filter is able to provide additional energy into the system while maintaining motion stability. This paper presents an approach inspired by the above method with modifications based on the specific operating range of the human finger. A feedback term is used to provide energy into a virtual dynamical system via spring displacement of the SEA. In addition, a nonlinear damping force is used to ensure that the system both does not exceed the physical range of the finger while ensuring stability during motion. In this regard, the system acts as a positive admittance controller by increasing the displacement of the wearer's finger as determined by the physical spring displacement.

The goal of this work is to provide an actuator design and control structure that facilitate improved gross hand motion by an impaired individual. Prediction algorithms, as shown in [22] could be used to analyze the motion and assist the user with more specific grasping actions. In this way, we hope to accomplish both general and unique finger motion to assist the wearer fully through the grasping motion.

2 SERIES ELASTIC ACTUATOR DESIGN AND INTEGRATION

To avoid the drawbacks of soft actuators, the entirety of the actuator should occupy a small volume, while having minimal weight. As such, the most reasonable location for the actuator within the exoskeleton is on the dorsum of the hand. The design of the SEA is shown in Fig. 1. The section view presented in Fig. 1a shows the key components of the design. The force transmission is accomplished through a leadscrew, driven by a DC motor and gearbox, that is connected to the output linkage by the compression springs. The pulling and pushing loads are transferred from the output linkage (1) to the front and back compression springs (2), respectively, into the leadscrew (3, 4) as indicated by Fig. 1b. A magnetic encoder is used to determine the position of the lead nut assembly as shown in dark grey in Fig. 1b. The assembled prototype is shown in Fig. 1c and has an envelope of 60 mm $\times$ 22 mm $\times$ 22 mm when the actuator is completely retracted. The mass of the assembled actuator is approximately 36 grams, fulfilling the lightweight requirement.

Utilizing a Pololu Micrometal Gearmotor with a 250:1 gear reduction and an output speed of 130 RPM, the system can travel the full 20mm in stroke required for closing the finger in approximately 0.659 seconds using a leadscrew with a 20 mm/rev lead. Considering the standard leadscrew lifting force calculation,

$$F_{raise} = \frac{2T}{\tan(\phi + \lambda) d_m} \tag{1}$$

The maximum linear force output of the SEA is 61 N after the springs become fully compressed. The chosen springs have a maximum working load of 44.5 N with a spring rate of 9.42 N/mm. In Eqn. (1), T is the actuator stall torque, ϕ is the angle of friction calculated as $\tan^{-1}(\mu_s)$ where μ_s is the static coefficient of friction between the leadscrew and nut, λ is the lead angle, and d_m is the leadscrew mean diameter.

The integration of the SEA with the finger linkage mechanism is shown in Fig. 2. Linear motion from the output linkage of the SEA is transmitted to the slotted member of the linkage mechanism via the slot shown in Fig. 2. The kinematic chain comprised of two serially connected four-bar mechanisms causes synchronized motion along the MCP, PIP, and DIP joints of the finger. The position of the finger is measured by a rotary potentiometer located at the MCP joint. For determining the compression of the elastic members in the SEA, rotation angle is converted to a corresponding linear position, x_{pot}, through

$$x_{pot} = \tan(\theta_{MCP}) h \tag{2}$$

where θ_{MCP} is the angle measured by the potentiometer and h is the vertical offset of the actuator from the sensor as shown in Fig. 2. The base of the SEA, indicated by the white members in Fig. 1b, is rigidly attached to the dorsum of the hand and considered

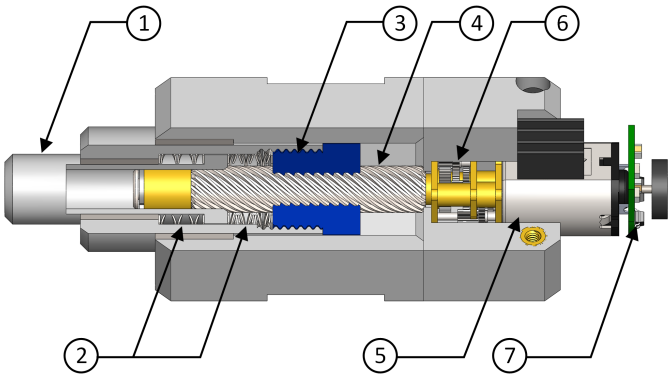

(a) The section view of the SEA module showing the 1) output linkage, 2) compression springs, 3) lead nut, 4) lead screw, 5) motor, 6) gearbox, and 7) magnetic encoder. The two load paths are indicated by the dashed red lines.

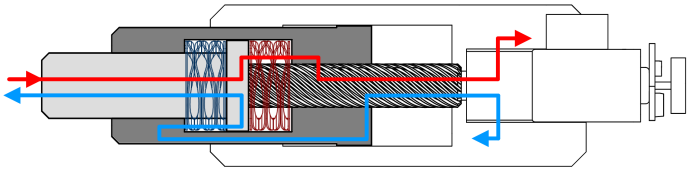

(b) The load path for pulling (bright blue) and pushing (bright red) loads that are transmitted through the output linkage (light grey) to the springs (dark blue and red, respectively) to the lead nut assembly (dark grey) down the lead screw into the base.

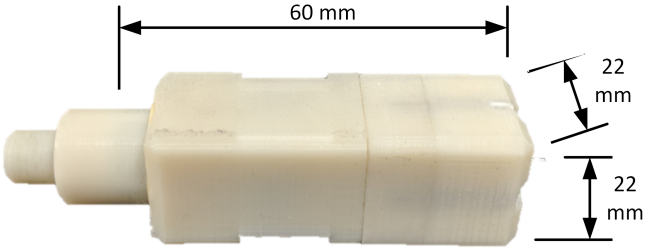

(c) The prototype of the SEA and its overall dimensions at its fully retracted position.

Figure 1: The SEA design overview.

fixed.

It should be noted that while determination of the user finger force is possible by measuring the spring compression, the purpose of the controller presented in the next section is to determine the user's motion intention, not force intention. In this way, the springs are a means to transmit force, not measure it. However, the design would allow such consideration in the future for a different control scheme.

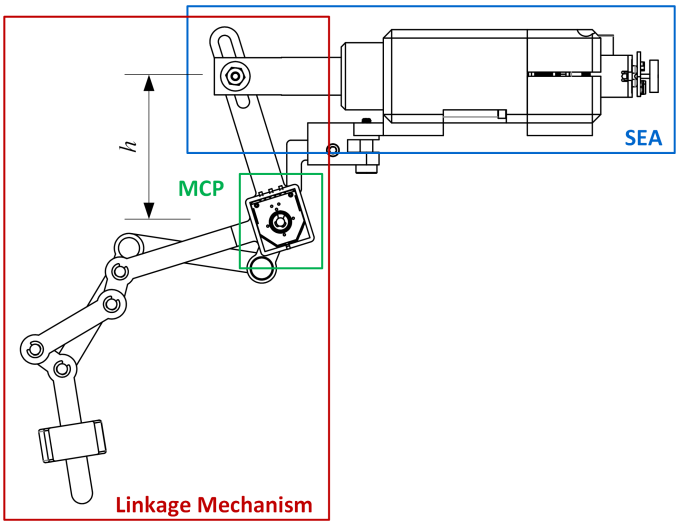

Figure 2: The layout of a single finger assembly with the actuator (blue) and linkage mechanism (red) with the potentiometer located at the MCP joint (green).

Table 1: The parameters for the SEA.

Parameter	Value
T	297 N-mm
ϕ	0.197 rad
μ_s	0.2
λ	0.858 rad
d_m	5.5 mm
l	20 mm/rev
η	1:250 rev/rev
h	30 mm

3 MOTOR CONTROL

The position of the actuator, x_1', is calculated from the rotation of the motor using

$$x_1' = \frac{l\eta\theta_m}{2\pi} \tag{3}$$

where l is the leadscrew lead, η is the gear reduction, and θ_m is the rotational position of the motor. Their values are also shown in Tab. 1.

A simple PD controller, running at a frequency of 1 kHz, was implemented to control x_1' on the prototype of the complete system shown in Fig. 2. It was implemented on a Teensy 3.2 microcontroller with a DRV8801 motor driver and a 12 count/rev magnetic encoder.

The results of the controller under a sinusoidal input are shown in Fig. 3. The input had a frequency near the edge of the motor's performance capabilities, to demonstrate the actua-

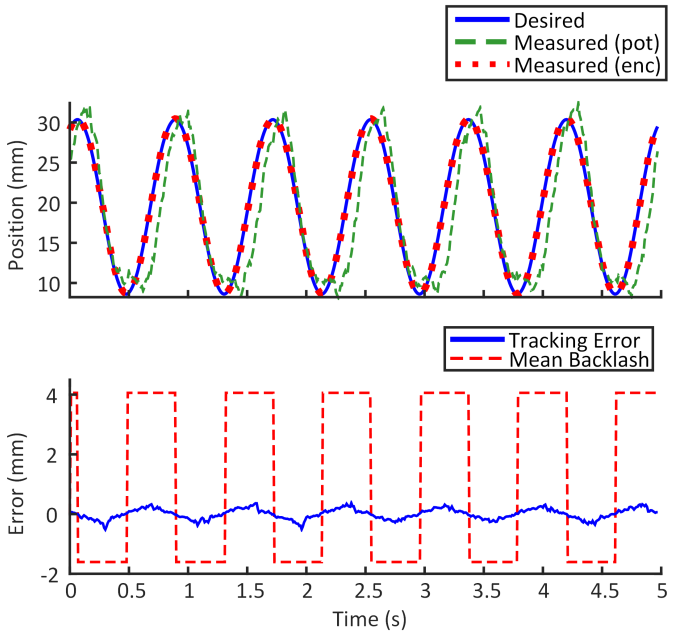

Figure 3: The tracking of the controller and the measured backlash in the system at the edge of the motor bandwidth.

tor motion bandwidth. It can be seen that this is in fact faster than the theoretical maximum actuator linear speed of 40 mm/s and the servo bandwidth of the system is 1.2 Hz at an amplitude of 20 mm. In addition, the corresponding values of x_{pot} are shown in green where no additional load was placed on the finger mechanism, measured using the Bourns 3382 rotary potentiometer. The error in the motor position tracking was less than 0.5 mm. The larger error between the x_{pot} and x_1', was averaged in the cases of positive and negative motor velocities and is shown in red in the second plot and can be used to characterize the backlash in the system. In the positive direction, the average backlash was 4.06 mm and in the negative direction it was 1.07 mm.

4 MOTION AMPLIFICATION CONTROL

To assist the motion of the user, a controller must be designed that behaves as though more energy was input into the SEA than actually was. Furthermore, the system must be able to quickly stop if an antagonistic motion is performed, while also stopping on its own in cases when the user may not have sufficient strength or control to stop the motion. As such, the higher level control of the finger mechanism is chosen according to

$$\begin{aligned} \dot{x_1} &= x_2 \\ \dot{x_2} &= -\alpha x_1 - b(\vec{x}) x_2 \quad \alpha > 0 \end{aligned} \tag{4}$$

The value for x_1 is the spring deflection determined as

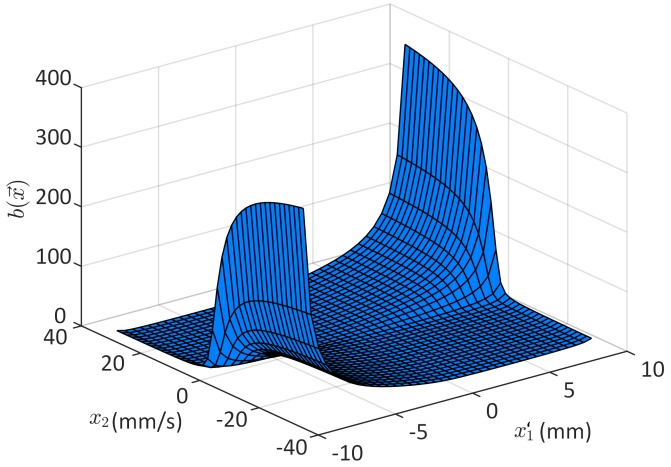

Figure 4: The damping manifold for the operating region of the actuator.

$x_{1ref}' - x_1'$ where x_1' is the position of the finger according to the encoder. In practice, x_{1ref}' is the same as x_{pot} and for purposes of modeling and motion stability analysis, chosen as a static value. The authors would again like to note that this is an important advantage of both this system design and control architecture. By estimating only the user's motion intent through a difference in the two position measurements, rather than user force, the level of uncertainty due to modeling errors is reduced. The user's intent will be defined by a non-zero value of x_1.

The damping, $b(\vec{x})$, is a strictly positive damping function, based on both the position and velocity of the finger, chosen as

$$b(\vec{x}) = \frac{\exp(\tan^{-1}(-x_1')\tan^{-1}(x_2))}{x_{1max}' - |x_1'|} \tag{5}$$

The above function was determined such that the damping becomes very large as the position of the finger moves towards the physical limit on either end. The manifold for the damping function is shown in Fig. 4. The value of x_{1max}' was chosen to be 5% larger than the true physical limit of the system as a factor of safety.

The stability of the controller can be shown by choosing the Lyapunov function candidate

$$V(\vec{x}) = \alpha \frac{x_1^2}{2} + \frac{x_2^2}{2} \tag{6}$$

where $V(\vec{x})$ is positive definite under the condition $\alpha > 0$ and its derivative is

$$\dot{V}(\vec{x}) = \alpha x_1 \dot{x_1} + x_2 \dot{x_2} \tag{7}$$

By substituting $\dot{x_1}$ and $\dot{x_2}$ from Eqn. (4),

$$\begin{aligned}\dot{V}(\vec{x}) &= \alpha x_1 x_2 + x_2(-\alpha x_1 - b(\vec{x})x_2) \\ &= -b(\vec{x})x_2^2 \leq 0\end{aligned} \tag{8}$$

The set $S = \{x_1, x_2 | \dot{V}(\vec{x}) = 0\}$ reduces to $S = \{x_1, x_2 | x_2 = 0\}$ as $b(\vec{x})$ is strictly positive. Since the only trajectory that causes S to be invariant is $x_1(t) = x_2(t) = 0$, by LaSalle's invariance principle, we can say the system is globally asympotically stable as $V(\vec{x})$ is radially unbounded in $\vec{x}$; however, as the system has bounds, it is stable within that domain. The bounds for the system are $x_1' \in [-10, 10]$ and $x_2 \in [-20, 20]$. The bounds for the system were enforced in software on top of the controller.

The response of the system was simulated using two cases, explained below, and the results of these simulations can be seen in Fig. 5 in which Eqn. (4) was numerically evaluated for 2 seconds in MATLAB. The first "drifting" case is when the user moves towards x_{1ref}' and then stops deflecting the spring once $x_1' = x_{1ref}'$. More explicitly,

$$x_1 = \begin{cases} x_{1ref}' - x_1' & \text{if } \text{sign}(x_{1ref}') = \text{sign}(x_{1ref}' - x_1') \\ 0 & \text{otherwise} \end{cases} \tag{9}$$

The case is designed to simulate a user who is trying to close their hand with varying strength, rather than trying to move their hand to a specific position. The response is shown in Fig. 5a for different values of x_{1ref}'. Manipulating the expression for $\dot{x}_2$ yields

$$\begin{aligned}\dot{x}_2(x_{1max} - |x_1'|) = &-\alpha x_1 (x_{1max} - |x_1'|) \\ &- \exp(\tan^{-1}(-x_1')\tan^{-1}(x_2))x_2\end{aligned} \tag{10}$$

where it can be seen that equilibrium positions exist when $x_1 = x_{1ref}' - x_1' = 0$ and $|x_1'| = x_{1max}'$. However, the latter is not achievable as $b(\vec{x})$ prevents it and $\lim_{t\to\infty} |x_1'| = x_{1max}'$. However, the response for two seconds is shown in Fig. 5a wherein a quantifiable increase in motion is present and shown in Fig. 6. The increase in motion as the $|x_{1ref}'| \to x_{1max}'$ asymptotically approaches unity.

The second "holding" case is when the user continuously tries to move to x_{1ref}'. As such, x_1 is always $x_{1ref}' - x_1'$ as opposed to the cases in Eqn (5). This response is much more reminiscent of a spring mass damper system as seen in Fig. 5b. Due to the persistent input from the user, the system reaches the closer equilibrium of $x_1' = x_{1ref}'$. As the position of the user, x_1', increases in magnitude, the damping ratio increases which leads to a change in behavior from under damped to over damped. This is reflected in the response when comparing $x_{1ref}' = x_{1max}'$ and $x_{1ref}' \ll x_{1max}'$.

The results of preliminary testing of the high level controller on the physical system shown in Fig. 7 are shown in Figs. 8a and 8b. Figure 7 shows the entire glove, but only a single finger is detailed as this is the focus of this work. The additional PCB shown on the actuator was not used in these experiments.

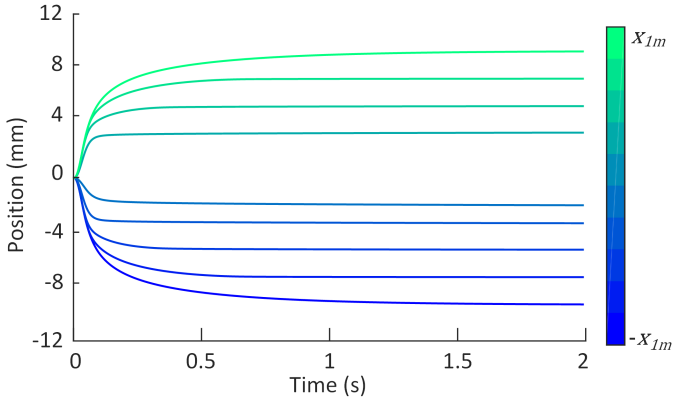

(a) The drifting case response.

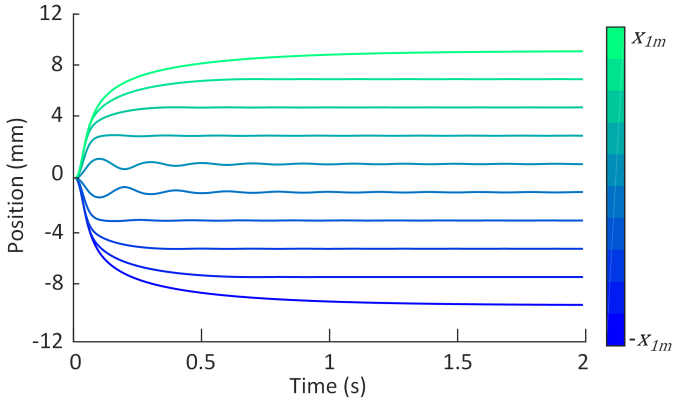

(b) The holding case response.

Figure 5: The simulated responses for the two types of input.

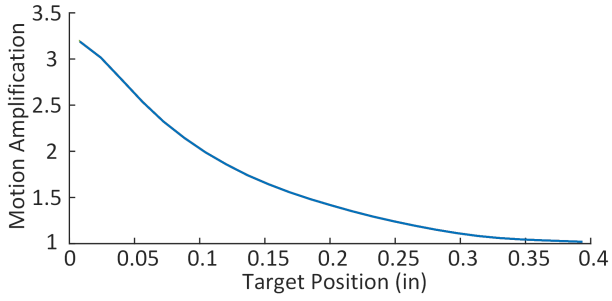

Figure 6: The increase in motion for the drifting case after two seconds.

Two "drifting" cases of large and small impulses were tested and their desired and measured positions of x_1' are shown in Fig. 8a where the impulses were delivered, manually, at 0.75 seconds and 1.1 seconds for the smaller and larger spring displace-

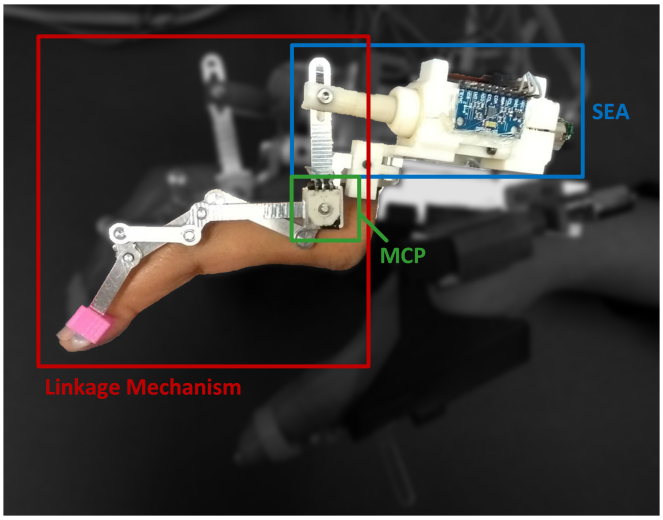

Figure 7: The prototype of the actuator and finger mechanism. The single digit assembly is shown in color with the actuator (blue), MCP joint sensor (green), and the linkage mechanism (red). The remainder of the prototype is not detailed as the focus of this work is on validating the single finger mechanism.

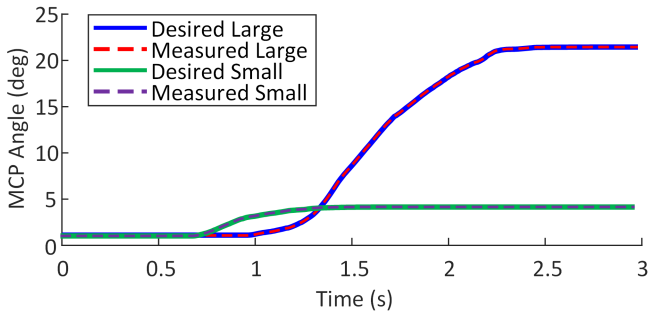

(a) The drifting case with a large and small input motion.

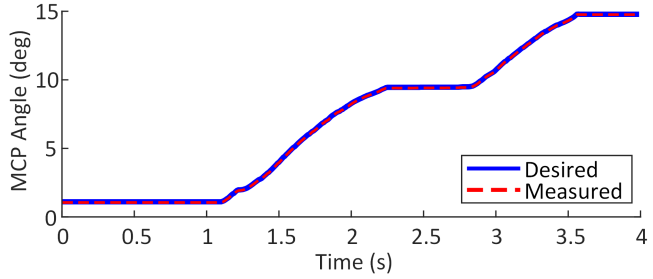

(b) The holding case with two target positions.

Figure 8: The experimental results of the motion amplification controller.

ments, respectively. The operator, in this case, moved a small or large amount and then relaxed their finger. It can be seen that the velocity of the system, x_2, naturally decreases to zero for the smaller motion but instantly decelerates as the limit on x_1' was enforced at the maximum desired range of motion.

The holding case is shown, with two discrete movements, in Fig. 8b. The motions were performed at 1.1 seconds and 2.2 seconds. The motion stops far more suddenly than in the drifting case as expected due to the operator attempting to move and then stop rather than move and stop applying resistance.

In both experiments, the motion is less smooth due to both the imperfect motion of the operator as well as clearly observable noise in the potentiometer as shown in Fig. 3. Furthermore, the motions shown are only for closing the finger due to the goal of the motion amplification as a means to facilitate sufficient motion for the grasp prediction algorithm.

5 CONCLUSION AND FUTURE WORK

This work presented the design of a compact SEA to actuate a linkage based mechanism for a hand exoskeleton. The low level motor controller was presented and evaluated with a maximum tracking error of less than 0.5 mm. In the same testing, the backlash between the actuator and the linkage mechanism was characterized. A high level motion planner was formulated as a virtual spring-mass-damper system with nonlinear damping to assist the motion of the user. The compliant elements in the SEA allow the user to provide a physical input into the system which is treated as a virtual spring displacement. The damping in the system becomes infinitely large at the maximum range of motion to gradually slow the user as they fully extend or contract their finger. The stability of the virtual dynamical system was proven and the response for two types of motion were shown in simulation and tested on a physical prototype.

The next stages of development of this actuator will involve the formal quantification of the motion amplification scheme as qualitative analysis with multiple human subjects wearing the device. Additionally, more ranges and types of motion will be tested such as small "holding" motions and following a trajectory. The actuator and controller will be integrated into a full prototype, along with a holistic grasp controller that uses the amplified motion to predict the grasping action the user is attempting [22]. The complete design will be made as light as possible to ensure portability and usability. Upon integration, the exoskeleton glove will be capable of full, start to finish grasp assistance.

ACKNOWLEDGMENT

Research reported in this publication was supported in part by the Eunice Kennedy Shriver National Institute of Child Health & Human Development of the National Institutes of Health under Award Number R21HD095027. The content is solely the responsibility of the authors and does not necessarily represent

the official views of the National Institutes of Health.

REFERENCES

[1] , 2017. National Health Interview Survey: Table A-10. Difficulties in physical functioning among adults aged 18 and over, by selected characteristics: United States, 2017. Tech. rep., U.S. Department of Health and Human Services, Centers for Disease Control and Prevention, National Center for Health Statistics.

[2] Wenzelburger, R., Kopper, F., Frenzel, A., Stolze, H., Klebe, S., Brossmann, A., Kuhtz-Buschbeck, J., Gölge, M., Illert, M., and Deuschl, G., 2005. "Hand coordination following capsular stroke". *Brain,* ***128***, pp. 64–74.

[3] , 2007. Impairments in motor execution. Tech. rep.

[4] Lang, C. E., DeJong, S. L., and Beebe, J. A., 2009. "Recovery of thumb and finger extension and its relation to grasp performance after stroke.". *Journal of neurophysiology,* ***102***(1), 7, pp. 451–9.

[5] SaeboFlex — Dynamic Finger Extension Orthosis for Grasping & Releasing.

[6] Yap, H. K., Jeong Hoon Lim, Nasrallah, F., Goh, J. C. H., and Yeow, R. C. H., 2015. "A soft exoskeleton for hand assistive and rehabilitation application using pneumatic actuators with variable stiffness". In 2015 IEEE International Conference on Robotics and Automation (ICRA), IEEE, pp. 4967–4972.

[7] Koo, I., Byunghyun Kang, B., and Cho, K.-J., 2013. "Development of Hand Exoskeleton using Pneumatic Artificial Muscle Combined with Linkage". *Journal of the Korean Society for Precision Engineering,* ***30***, pp. 1217–1224.

[8] Polygerinos, P., Lyne, S., Wang, Z., Nicolini, L. F., Mosadegh, B., Whitesides, G. M., and Walsh, C. J., 2013. "Towards a soft pneumatic glove for hand rehabilitation". *IEEE International Conference on Intelligent Robots and Systems*, pp. 1512–1517.

[9] Polygerinos, P., Wang, Z., Galloway, K. C., Wood, R. J., and Walsh, C. J., 2015. "Soft robotic glove for combined assistance and at-home rehabilitation". *Robotics and Autonomous Systems,* ***73***, pp. 135–143.

[10] Yun, S.-S., Kang, B. B., and Cho, K.-J., 2017. "Exo-Glove PM: An Easily Customizable Modularized Pneumatic Assistive Glove". *IEEE Robotics and Automation Letters,* ***2***(3), pp. 1725–1732.

[11] SangWook Lee, Landers, K. A., and Hyung-Soon Park, 2014. "Development of a Biomimetic Hand Exotendon Device (BiomHED) for Restoration of Functional Hand Movement Post-Stroke". *IEEE Transactions on Neural Systems and Rehabilitation Engineering,* ***22***(4), 7, pp. 886–898.

[12] In, H., and Cho, K.-j., 2015. "Exo-Glove : Soft wearable robot for the hand using soft tendon routing system". *IEEE Robotics & Automation,* ***22***(March 2015), pp. 97–105.

[13] Nycz, C. J., Delph, M. A., and Fischer, G. S., 2015. "Modeling and design of a tendon actuated soft robotic exoskeleton for hemiparetic upper limb rehabilitation". *Proceedings of the Annual International Conference of the IEEE Engineering in Medicine and Biology Society, EMBS,* ***2015-Novem***, pp. 3889–3892.

[14] Popov, D., Gaponov, I., and Ryu, J.-H., 2017. "Portable Exoskeleton Glove With Soft Structure for Hand Assistance in Activities of Daily Living". *IEEE/ASME Transactions on Mechatronics,* ***22***(2), 4, pp. 865–875.

[15] Ma, Z., and Ben-Tzvi, P., 2013. "Tendon transmission efficiency of a two-finger haptic glove". *ROSE 2013 - 2013 IEEE International Symposium on Robotic and Sensors Environments, Proceedings*, pp. 13–18.

[16] Belter, J. T., and Dollar, A. M., 2013. "Novel differential mechanism enabling two DOF from a single actuator: Application to a prosthetic hand". In 2013 IEEE 13th Int. Conf. on Rehabilitation Robotics (ICORR), IEEE, pp. 1–6.

[17] Úbeda, A., Zapata-Impata, B. S., Puente, S. T., Gil, P., Candelas, F., and Torres, F., 2018. "A vision-driven collaborative robotic grasping system tele-operated by surface electromyography". *Sensors (Switzerland),* ***18***(7).

[18] Noronha, B., Dziemian, S., Zito, G. A., Konnaris, C., and Faisal, A. A., 2017. "'Wink to grasp' - Comparing eye, voice & EMG gesture control of grasp with soft-robotic gloves". In IEEE International Conference on Rehabilitation Robotics.

[19] Refour, E., Sebastian, B., and Ben-Tzvi, P., 2018. "Two-Digit Robotic Exoskeleton Glove Mechanism: Design and Integration". *Journal of Mechanisms and Robotics,* ***10***(2), p. 025002.

[20] Vanteddu, T., Sebastian, B., and Ben-Tzvi, P., 2018. "Design Optimization of RML Glove for Improved Grasp Performance". In Proceedings of the ASME 2018 Dynamic Systems and Control Conf. (DSCC 2018), pp. 1–8.

[21] Nagarajan, U., Aguirre-Ollinger, G., and Goswami, A., 2016. "Integral admittance shaping: A unified framework for active exoskeleton control". *Robotics and Autonomous Systems,* ***75***, 1, pp. 310–324.

[22] Chauhan, R. J., and Ben-Tzvi, P., 2018. "Latent Variable Grasp Prediction for Exoskeletal Glove Control". In ASME Dynamic Systems and Control.